



Carbon paper coated with supported tungsten trioxide as novel electrode for all-vanadium flow battery

Chuan Yao^{a,b}, Huamin Zhang^{a,*}, Tao Liu^a, Xianfeng Li^a, Zonghao Liu^c

^a Division of Energy Storage, Dalian Institute of Chemical Physics, Chinese Academy of Sciences, Dalian 116023, China

^b Graduate School of Chinese Academy of Sciences, Beijing 100039, China

^c Dalian Rongke Power Co. Ltd., Dalian 116025, China

H I G H L I G H T S

- ▶ Carbon paper coated with WO₃/SAC work as novel modified electrodes of VFB.
- ▶ Electrochemical performances of the modified electrode are improved.
- ▶ Charge transfer resistances on the modified electrode are reduced significantly.
- ▶ The increased performance is attributed to the synergistic effect of WO₃ and SAC.

A R T I C L E I N F O

Article history:

Received 9 January 2012

Received in revised form

20 June 2012

Accepted 21 June 2012

Available online 13 July 2012

Keywords:

Vanadium redox flow battery
Tungsten trioxide/super activated carbon
Carbon paper
Electrochemical performance
Voltage efficiency

A B S T R A C T

A novel carbon paper electrode coated with supported tungsten trioxide is developed to improve the carbon fiber's electrochemical performance toward the vanadium redox couples. Super activated carbon supported tungsten trioxide (WO₃/SAC) is prepared via an impregnation method and characterized by X-ray diffraction and scanning electron microscopy. The electrochemical performance of the prepared electrode is evaluated with cyclic voltammetry and electrochemical impedance spectroscopy. Results show that WO₃/SAC exhibits excellent electro-catalytic activity and kinetic reversibility toward the vanadium redox couples. By adding the WO₃/SAC, the charge transfer resistances for both the positive and the negative reactions are significantly reduced. Using as prepared electrodes, the coulombic efficiency (CE), voltage efficiency (VE) and energy efficiency (EE) of the vanadium redox flow battery at 50 mA cm⁻² are 94.5%, 85.2% and 80.5%, respectively, which are much higher than that of the cell assembled with pristine carbon paper electrodes.

© 2012 Elsevier B.V. All rights reserved.

1. Introduction

Redox flow batteries (RFB) are electrochemical energy conversion and storage devices based on electrochemical changes of redox couples in a cycled flowing liquid [1]. RFB system is considered to be ideal for large scale energy storage, due to its advanced characteristics such as high energy conversion efficiency, high reliability, long cycle life, flexible design, fast response, and low operation and maintenance costs [2–4]. RFB can be used to store intermittent electricity generated by renewable energy sources such as wind and solar power for smooth and stable output. It is also an important element in the smart grid, functioning as load leveling device, uninterruptible power system (UPS), reserve

power, etc. [5–8]. Among various kinds of RFB, all vanadium flow battery (VFB) is a promising and the most developed one, which employs V(II)/V(III) and V(IV)/V(V) as the negative and positive redox couples, respectively, with the standard open circuit cell potential approximate 1.26 V [5,9]. Due to the usage of the same metal element in both side electrolytes, the cross-contamination which leads to the cell performance degradation is significantly decreased [8].

Typical electrode materials for VFB are carbon materials such as carbon felt, graphite felt and carbon paper. The advantages of these materials are their suitable porosity, high surface area, wide operation potential range, and low cost [10]. However, the pristine carbon materials still show poor kinetic reversibility [8]. Considerable studies on the modification of the electrode materials have been carried out to enhance their electrochemical performance, those methods include ion exchange [11], heat or acid treatment [12,13], electrochemical oxidation [14], metal deposition [8,15], etc.

* Corresponding author. Tel.: +86 411 84379072; fax: +86 411 84665057.
E-mail address: zhanghm@dicp.ac.cn (H. Zhang).

Recently, Lu Yue et al. reported a highly hydroxylated carbon paper prepared by ultrasonic treating in mixed acids. Used as VFB electrodes, the energy efficiency of the cell achieved to 75.1% at 10 mA cm^{-2} [16]. Carboxyl multi-walled carbon nanotubes (MWCNTs) as electrochemical active materials for $\text{VO}^{2+}/\text{VO}_2^+$ redox couple were studied. Using the carboxyl MWCNTs/carbon felt as VFB positive electrode, the cell performance was improved, the CE, VE and EE were 98.6%, 76.1% and 75.0%, respectively at 70 mA cm^{-2} [17].

In this study, a novel modification method, using tungsten oxide (WO_3)/super activated carbon (SAC) composite to coat the carbon paper, is presented. Tungsten oxide is an interesting inorganic metal oxide, and has attracted much attention due to its excellent properties in electrochemical devices, solar cells, gas sensors and catalysts [18–21]. Additional advantages of WO_3 are facile preparation, stable in sulfuric acid and low cost compared to other metal oxides like IrO_2 or RuO_2 , which used to be employed as VFB electrode materials. This is the first time that WO_3 has been applied to reaction catalyst for VFB. SAC is provided with high surface area, good electrical conductivity, and is catalytically active toward vanadium redox couples. Therefore, it suits for the support of WO_3 . The WO_3 /SAC composite used as a modifier to the electrode material was prepared through an impregnation method. Surface morphology and crystal structure were analyzed by means of SEM and XRD. Cyclic voltammetry (CV) and electrochemical impedance spectroscopy (EIS) were employed to evaluate the electrochemical activity of the as prepared electrodes. Finally, dynamic flowing single cell test was carried out.

2. Experimental

2.1. Materials and chemicals

Chemicals used in this study were: $(\text{NH}_4)_6\text{W}_7\text{O}_{24} \cdot 6\text{H}_2\text{O}$ (Tianjin Institute of Fine Chemicals, China), $\text{VOSO}_4 \cdot n\text{H}_2\text{O}$ (VOSO_4 , 70 wt.%, Dalian Bolong Invest Co., Ltd, China), H_2SO_4 (98 wt.%, Jinzhou Gucheng Chemical Reagent, China), anhydrous alcohol (Tianjin Concord Technology Co., Ltd, China). All chemicals were analytical reagent grade and were directly used without further purification. Super activated carbon (surface area: $2900 \text{ m}^2 \text{ g}^{-1}$, pore cubage: 1.588 mL g^{-1}) and carbon paper were purchased from Jinzhou Changhong Petrochemical Co., Ltd, China and SGL Carbon AG, Germany, respectively. Nafion115 ion exchange membrane and 5 wt.% Nafion solution were obtained from Dupont, USA.

2.2. Preparation of electrode

50 mg $(\text{NH}_4)_6\text{W}_7\text{O}_{24} \cdot 6\text{H}_2\text{O}$ was firstly dissolved in 30 mL ethanol–deionized water mixed solution (V/V 2:1), and then 50 mg super activated carbon powder was added and ultra-sonicated to homogeneous dispersion for 2 h at room temperature. Afterward, the solvent was evaporated at 80°C with vigorous stirring. The resultant product was dried at 100°C for 12 h in vacuum oven and treated at 550°C for 2 h in N_2 . After cooling to room temperature, the product was grinded in agate bowl to obtain the WO_3 /SAC powder.

The WO_3 /SAC powder and 5 wt.% Nafion solution (the mass ratio of WO_3 /SAC and Nafion was 3:1) were put into appropriate volume of anhydrous alcohol, sonicated for 30 min to get fully dispersed suspension. Carbon paper was cut into proper size and was coated with WO_3 /SAC suspension by means of spray gun, with a loading of 0.75 mg cm^{-2} on each side of the carbon paper.

2.3. Physical characterization and electrochemical tests

The crystal structure of WO_3 /SAC powder was characterized by X-ray diffraction (PANalytical X'pert PRO). The morphology of the

WO_3 /SAC powder was examined using a JSM-6360LV scanning electron microscopy (SEM).

The electrochemical activity of as prepared electrode was evaluated by cyclic voltammetry (CV) and electrochemical impedance spectroscopy (EIS). CV results were obtained on the CHI600b (CH Instruments, USA) workstation. EIS was measured on the PARSTAT 2273 (Princeton Applied Research, USA) by applying an alternating voltage of 5 mV over the frequency ranging from 10^{-1} to 10^5 Hz . For electrochemical test, a three-electrode system was utilized with carbon paper as the working electrode, a saturated calomel electrode (SCE) as the reference electrode and the graphite plate as the counter electrode. Structure of the working electrode was shown in Fig. 1. A piece of carbon paper was sandwiched between two plastic sheets, on one of which there was an open circular hole of 0.785 cm^2 as the working area. A piece of Cu foil contacted to the carbon paper served as the current collector.

The investigation of positive redox couple V(IV)/V(V) and negative redox couple V(II)/V(III) was carried out in $0.05 \text{ M V(IV)} + 0.05 \text{ M V(V)} + 3 \text{ M H}_2\text{SO}_4$ solution and $0.05 \text{ M V(II)} + 0.05 \text{ M V(III)} + 3 \text{ M H}_2\text{SO}_4$ solution, respectively. The V(IV) solution was prepared by dissolving $\text{VOSO}_4 \cdot n\text{H}_2\text{O}$ in hot H_2SO_4 solution, other V solutions with different valance states (II, III, V) were obtained by electrolyzing the as prepared V(IV) solution. Due to V(II) is sensitive to air and easily oxidized to V(III) , N_2 was introduced into the electrolyte to keep an inert atmosphere during the investigation. Carbon paper coated with WO_3 /SAC, carbon paper coated with SAC (heat treatment at 550°C for 2 h, loading of 0.75 mg cm^{-2} on each side) and the pristine carbon paper were evaluated, respectively.

2.4. Single cell evaluation

Constant current charge–discharge test was carried out using a single cell on a battery test system SIN 164867-A Arbin instrument (Arbin Co., USA). Two pieces of carbon paper with an active area of 9 cm^2 ($3.0 \text{ cm} \times 3.0 \text{ cm}$) were used as positive and negative electrodes, respectively. Nafion115 ion exchange membrane was

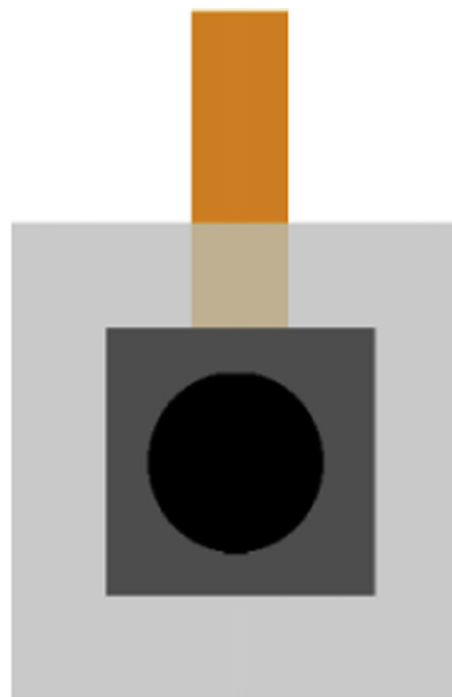


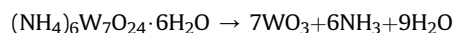
Fig. 1. Sketch map of working electrode.

employed as the separator. Graphite plate with serpentine flow field on its surface served as the current collector. The cell was sealed with rubber washers. The initial positive and negative electrolytes were 30 mL 1.5 M V(IV) + 3 M H₂SO₄ and 30 mL 1.5 M V(III) + 3 M H₂SO₄, which were stored in tanks outside the cell. When cell running, the electrolytes were pumped into the compartments as cycled flowing liquid. The upper limit of charge voltage and the lower limit of discharge voltage were 1.65 and 0.8 V. Three cells with different electrodes of the pristine carbon paper, the carbon papers coated with SAC and WO₃/SAC were investigated, denoted as cell A, B and C, respectively.

3. Results and discussion

3.1. SEM and XRD survey for WO₃/SAC

Fig. 2 shows the surface morphology of SAC and WO₃/SAC. It can be seen that SAC particles are irregular sheets with many arris edges. After WO₃ loading, the tiny snow like WO₃ particles disperse around SAC particles. The characterization results of crystal structure were shown in Fig. 3. For SAC, XRD pattern only exhibits two weak carbon peaks, the (002) peak located at 24.1° and (101) peak located at 43.0°. For WO₃/SAC powder, the characteristic diffraction peaks of WO₃ appeared. The significant diffraction peaks located at 23.08°, 24.10°, 28.78°, 33.64°, 34.05°, 41.52°, 55.40° indicate the presence of WO₃ with a crystal structure of orthorhombic [22]. The mechanism of thermal decomposition of (NH₄)₆W₇O₂₄·6H₂O at 550 °C to form WO₃ under nitrogen can be assumed as following:



3.2. Cyclic voltammetry analysis

Fig. 4 presents the CV curves of V(IV)/V(V) and V(II)/V(III) redox couples on different carbon paper electrodes. In Fig. 4(a), the redox reaction of V(IV)/V(V) couple can be detected on three electrodes in the sweeping voltage range of 0.3–1.2 V vs. SCE. The anodic peak O1 and the cathodic peak R1 correspond to the oxidation and the reduction processes, respectively. The detailed parameters obtained from the CV curves were listed in Table 1. For the pristine carbon paper, the shapes of the oxidation peak and the reduction peak are unsymmetrical, and the corresponding currents I_{pa} and I_{pc} are small, indicating that the electrochemical activity is relatively low. When the carbon paper is coated with SAC, both oxidation and reduction peak currents are increased remarkably and the peak potential separation is decreased from 311 mV to 151 mV, suggesting that the electrochemical activity and the kinetic reversibility on this electrode are improved compared with the

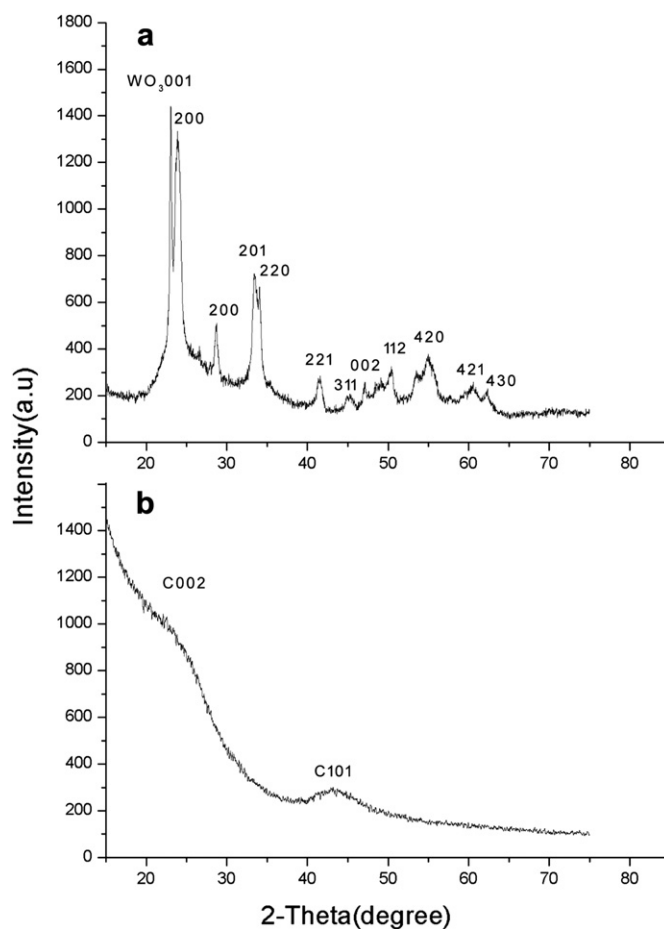


Fig. 3. XRD patterns of WO₃/SAC (a) and SAC (b).

pristine one. When the carbon paper is coated with WO₃/SAC, the peak currents are further increased, the magnitudes of which are almost the same (I_{pa}/I_{pc} is close to 1.03). The peak potential separation is only 106 mV, meaning that the kinetic reversibility is further improved as well.

CV performances on the three electrodes for the negative redox couple were shown in Fig. 4(b). The sweeping voltage was from −0.7 to −0.2 V vs. SCE. In this range, no obvious redox peak was detected on the pristine carbon paper electrode, indicating that the electrochemical performance toward V(II)/V(III) is quite inferior. When the carbon paper was coated with SAC, the oxidation

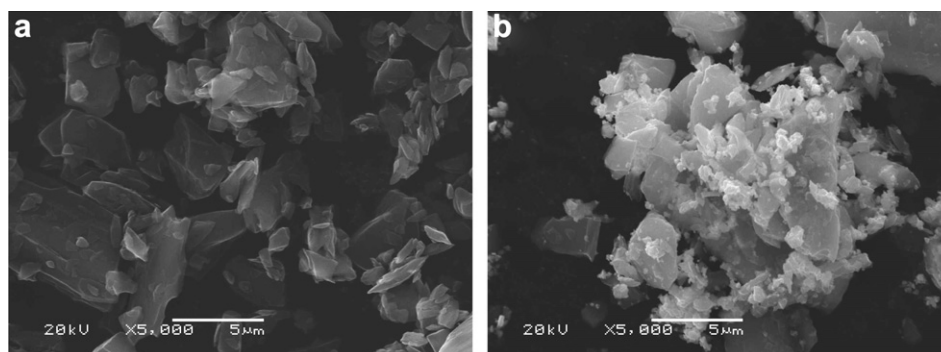


Fig. 2. Surface morphology of SAC powder (a) and WO₃/SAC powder (b).

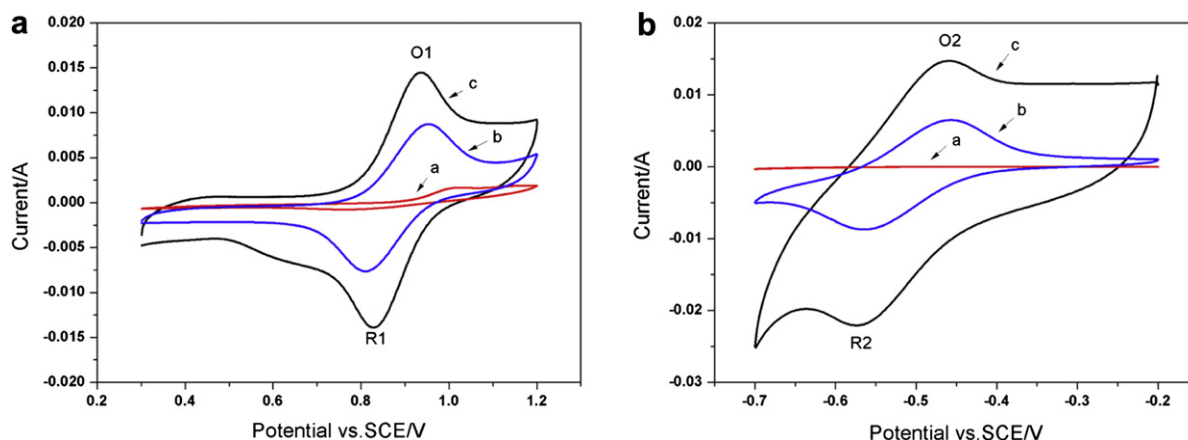


Fig. 4. CV curves of carbon paper a, carbon paper coated with SAC b, and carbon paper coated with WO_3/SAC c, at a scan rate of 10 mV s^{-1} in $0.05 \text{ M V(IV)} + 0.05 \text{ M V(V)} + 3 \text{ M H}_2\text{SO}_4$ solution (a) and $0.05 \text{ M V(II)} + 0.05 \text{ M V(III)} + 3 \text{ M H}_2\text{SO}_4$ solution (b).

Table 1
Parameters obtained from CV curves for the V(IV)/V(V) redox couple.

Electrode	E_{pa} (V)	E_{pc} (V)	I_{pa} (mA)	I_{pc} (mA)	ΔE_p (mV)	I_{pa}/I_{pc}
Pristine carbon paper	1.073	0.762	1.84	0.89	311	2.07
Carbon paper coated with SAC	0.959	0.808	8.85	7.76	151	1.14
Carbon paper coated with WO_3/SAC	0.934	0.828	14.49	14.02	106	1.03

peak O2 and reduction peak R2 become clear, locating at -0.50 to -0.45 V and -0.60 to -0.55 V , respectively. The peak voltage separation is around 110 mV . Compared with the carbon paper coated with SAC, the peak position of the carbon paper coated with WO_3/SAC electrode is almost no change; however, both the oxidation and reduction peak currents achieve an approximate two-fold increase.

Fig. 5 shows the CV curves of V(II)/V(III) and V(IV)/V(V) redox couples on carbon paper coated with WO_3/SAC at different scan rates. With the scan rate increasing, the peak potential separation changes little, suggesting the redox reactions on V(II)/V(III) and V(IV)/V(V) couples are quasi-reversible on this electrode. In summary, the electrode of carbon paper coated with WO_3/SAC exhibits the excellent electrochemical properties toward both positive and negative redox couples for VFB.

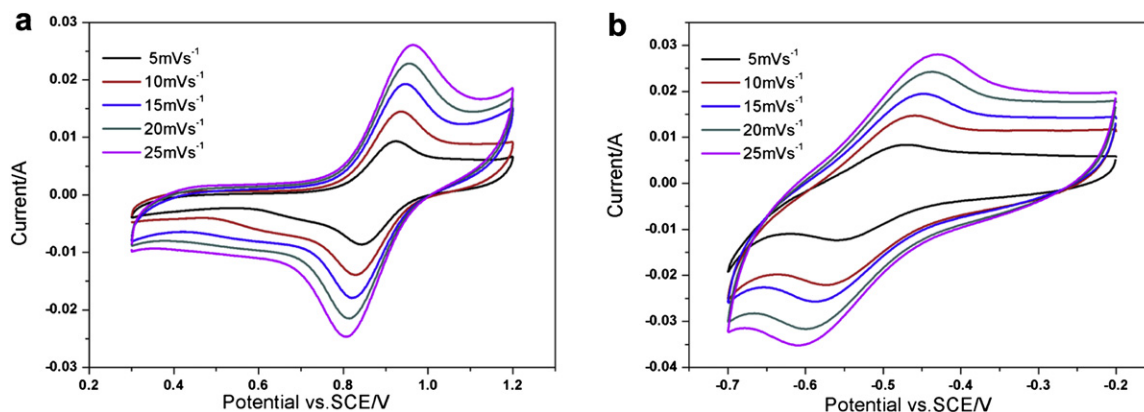


Fig. 5. CV curves of carbon paper coated with WO_3/SAC under different scan rates in $0.05 \text{ M V(IV)} + 0.05 \text{ M V(V)} + 3 \text{ M H}_2\text{SO}_4$ solution (a) and $0.05 \text{ M V(II)} + 0.05 \text{ M V(III)} + 3 \text{ M H}_2\text{SO}_4$ solution (b).

3.3. Electrochemical impedance spectroscopy

Fig. 6(a–c) displays a series of Nyquist plots obtained in $0.05 \text{ M V(IV)} + 0.05 \text{ M V(V)} + 3 \text{ M H}_2\text{SO}_4$ solution at 0.9 V vs. SCE for the three electrodes. All the Nyquist plots include a semicircle part at high frequency and a linear part at low frequency, suggesting that the V(IV)/V(V) redox reaction is mix-controlled by charge transfer and diffusion steps [16]. The high frequency semi-arc arose from the charge transfer reaction at the electrolyte/electrode interface. The radius of the semi-arc reflects the charge transfer resistance. The low frequency linear part can be attributed to the diffusion processes associated with VO_2^+ and VO^{2+} ions through the solution. It can be seen from Fig. 6 that the magnitude of high frequency semi-arc becomes smaller when SAC or WO_3/SAC was coated on carbon paper. The carbon paper coated with WO_3/SAC has the smallest semi-arc radius, indicating that the catalysis of WO_3/SAC can efficiently reduce the charge transfer resistance.

EIS results for negative redox couple are shown in Fig. 6(d–f). The investigation was carried out in $0.05 \text{ M V(II)} + 0.05 \text{ M V(III)} + 3 \text{ M H}_2\text{SO}_4$ solution at -0.55 V vs. SCE . For the pristine carbon paper electrode and the carbon paper coated with SAC electrode, the Nyquist plots only include a semicircle part, indicating that the V(II)/V(III) redox reaction is controlled by charge transfer in the entire frequency range, whereas, the charge transfer resistance is still significantly decreased when SAC was coated on the carbon paper. Since the catalysis of WO_3/SAC facilitates the

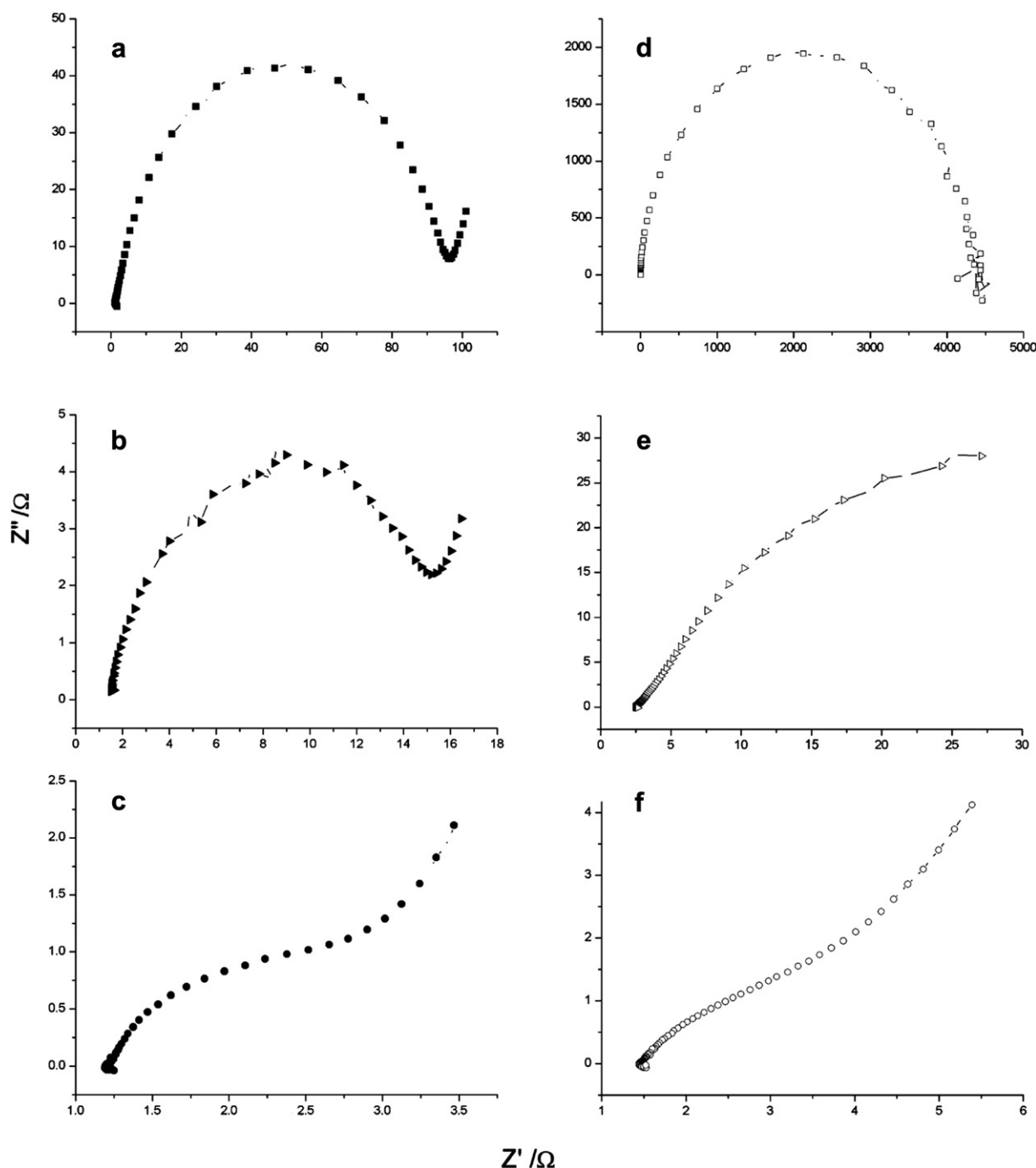


Fig. 6. AC impedance spectroscopy of carbon paper (a), carbon paper coated with SAC (b), carbon paper coated with WO_3/SAC (c) in 0.05 M V(IV) + 0.05 M V(V) + 3 M H_2SO_4 solution at 0.9 V vs. SCE and carbon paper (d), carbon paper coated with SAC (e), carbon paper coated with WO_3/SAC (f) in 0.05 M V(II) + 0.05 M V(III) + 3 M H_2SO_4 solution at -0.55 V vs. SCE.

V(II)/V(III) redox reaction, charge transfer resistance is further reduced and no longer the control step in low frequency range. Comparing Fig. 6(a), (b), (c) with (d), (e), (f), it can be found that each electrode has larger charge transfer resistance for V(II)/V(III) redox reaction than that for V(IV)/V(V) redox reaction, which is consistent with the test results from CV.

3.4. VFB single cell performance

Fig. 7 presents the charge–discharge curves of three cells assembled with the pristine carbon paper, and carbon papers

coated with SAC and WO_3/SAC , at a current density of 50 mA cm^{-2} . It can be seen that the curve of the cell C using carbon paper coated with WO_3/SAC as its electrode has a lowest charge voltage plateau and a highest discharge voltage plateau, thereby achieving the highest voltage efficiency, since the catalysis of WO_3/SAC reduces the electrochemical polarization of the positive and negative redox reaction. For the same reason, cell C obtains higher charge and discharge capacities. The detailed data obtained from Fig. 7 were summarized in Table 2. The voltage efficiency and the energy efficiency of cell C are 85.2% and 80.5% at the current density of 50 mA cm^{-2} , which is the best among the three cells.

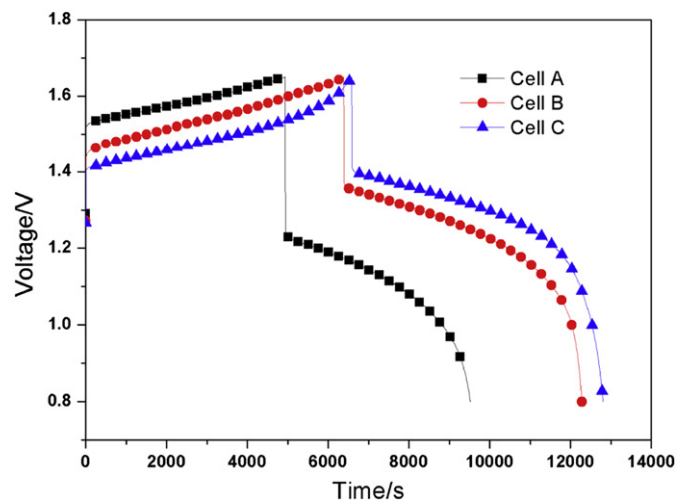


Fig. 7. Charge–discharge profiles of the cell A, B and C at the current density of 50 mA cm^{-2} .

Table 2

Parameters obtained from fitting the charge and discharge curves of Fig. 7 at the current density of 50 mA cm^{-2} .

Cells	Initial charge voltage (V)	Initial discharge voltage (V)	Voltage efficiency (%)	Charge capacity (mA h)	Discharge capacity (mA h)
A	1.516	1.240	69.7	598.0	558.7
B	1.431	1.373	79.5	797.0	734.9
C	1.399	1.411	85.2	821.4	777.2

Typical charge–discharge curves of cell C at current densities of $30, 40, 50$ and 60 mA cm^{-2} were tested and presented in Fig. 8. It can be found that the cell maintains good charge–discharge performance at different current densities. The efficiencies of cell C were listed in Table 3. At 30 mA cm^{-2} , the CE, VE and EE are 91.1%, 91.2% and 83.1%, respectively. Even the current density reaches to 60 mA cm^{-2} , the VE still stays upper than 80%. Fig. 9 presents the energy efficiency data of 50 times charge–discharge cycles of cell C at 30 mA cm^{-2} . There is almost no performance degradation. It suggests that the WO_3/SAC particles bonded with Nafion could enduringly stay on the carbon paper surface under the flowing electrolyte.

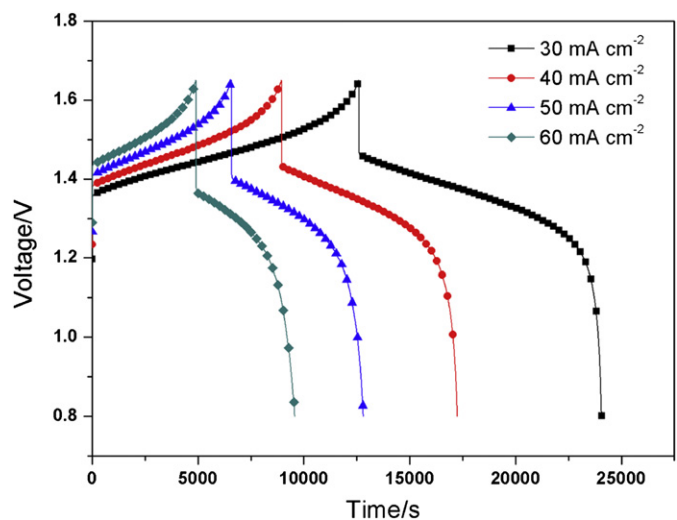


Fig. 8. Charge–discharge profiles of cell C at current densities of $30, 40, 50$ and 60 mA cm^{-2} .

Table 3

Efficiencies of cell C at current densities of $30, 40, 50$ and 60 mA cm^{-2} .

Current density (mA cm^{-2})	Coulombic efficiency (%)	Voltage efficiency (%)	Energy efficiency (%)
30	91.1	91.2	83.1
40	93.0	88.3	82.1
50	94.5	85.2	80.5
60	95.1	81.8	78.1

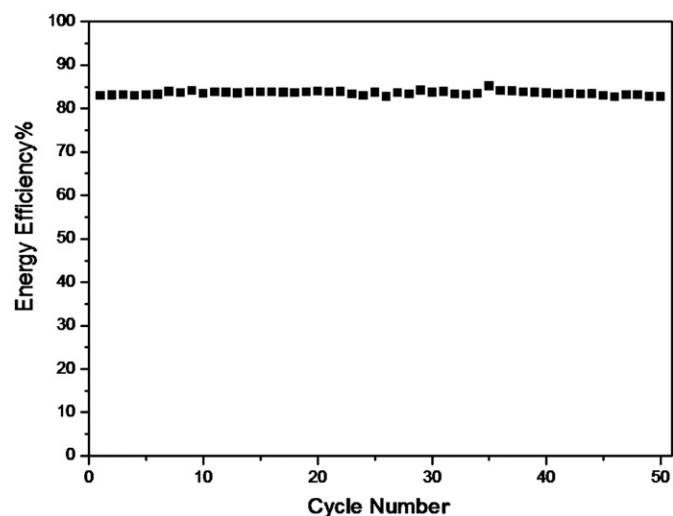


Fig. 9. The energy efficiency data of 50 charge–discharge cycles of cell C at 30 mA cm^{-2} .

3.5. The catalytic mechanism

CV and EIS results suggest that the improved electrode catalytic activities can be attributed to the synergistic effect of WO_3 and SAC. SAC is a kind of amorphous carbon with high surface area and large pore cubage. The characteristic diffraction peaks of SAC are broad and weak, which means the crystal degree is low. There would be lots of unsaturated carbon atoms exposed on the particle surface serving as active sites. Therefore, carbon paper coated with SAC possesses a higher electrochemical performance than the pristine one. Due to the poor conductivity, WO_3 is not suitable to work solely as an electrode. When composited with SAC, the conductivity and the dispersing are improved. The functional group $-\text{W}^{6+}=\text{O}$ on the surface of WO_3 molecule may be the key factor for the remarkable improvement of electrochemical activities [23]. The catalytic mechanism is presumed as shown in Fig. 10. In short, SAC provides large electrode surface area, good conductivity and parts of the active sites. WO_3 supplies more active center to improve the absorption ability of activated species and decrease the polarization of electrode reactions, so the composite WO_3/SAC exhibited excellent electrochemical activity toward the $\text{V(II)}/\text{V(III)}$ and $\text{V(IV)}/\text{V(V)}$ redox couples.

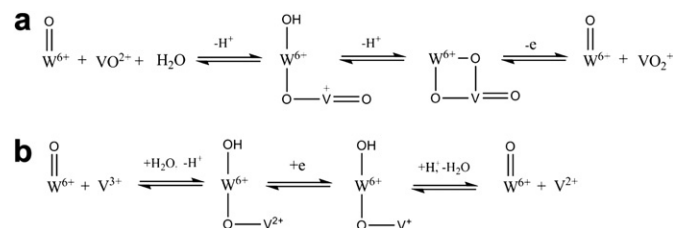


Fig. 10. The presumed catalytic mechanism of WO_3/SAC toward $\text{VO}^{2+}/\text{VO}_2^+$ (a) and $\text{V}^{2+}/\text{V}^{3+}$ (b) couples.

4. Conclusions

Carbon paper is coated with WO₃/SAC to improve the electrochemical performance toward vanadium redox couples at the electrode. The electrochemical activity and the kinetic reversibility of as prepared electrode are improved, and the charge transfer resistance is reduced significantly. The increased activity can be attributed to the synergistic effect of super activated carbon and tungsten trioxide. The single cell performance is improved remarkably by using WO₃/SAC coated carbon paper electrode. At a current density of 50 mA cm⁻², the CE, VE and EE of the cell are 94.5%, 85.2% and 80.5%, respectively, which are much higher than those of the cell assembled with the pristine carbon paper. After 50 cycles' charge–discharge durability test at 30 mA cm⁻², no energy efficiency attenuation is observed.

Acknowledgments

This work is financially supported by National Basic Research Program of China (No. 2010CB227203).

References

- [1] I. Tsuda, K. Nozaki, K. Sakuta, K. Kurokawa, *Sol. Energy Mater. Sol. Cells* 47 (1997) 101–107.
- [2] C. Poncedo de León, A. Frías-Ferrer, J. González-García, D.A. Szánto, F.C. Walsh, *J. Power Sources* 160 (2006) 716–732.
- [3] M. Skyllas-Kazacos, M. Rychcik, R.G. Robins, A.G. Fane, *J. Electrochem. Soc.* 133 (1986) 1057–1058.
- [4] F. Rahman, M. Skyllas-Kazacos, *J. Power Sources* 189 (2009) 1212–1219.
- [5] M. Gattrell, J. Park, B. MacDougall, J. Apte, S. McCarthy, C. Wu, *J. Electrochem. Soc.* 151 (2004) 123–130.
- [6] L. Joerissen, J. Garche, C. Fabjan, G. Tomazic, *J. Power Sources* 127 (2004) 98–104.
- [7] G. Orij, G.Y. Katayama, T. Miura, *J. Power Sources* 139 (2005) 321–324.
- [8] W.H. Wang, X.D. Wang, *Electrochim. Acta* 52 (2007) 6755–6762.
- [9] P. Qian, H.M. Zhang, J. Chen, Y.H. Wen, Q.T. Luo, Z.H. Liu, D.J. You, B.L. Yi, *J. Power Sources* 175 (2008) 613–620.
- [10] H. Kaneko, K. Nozaki, Y. Wada, T. Aoki, A. Negishi, M. Kamimoto, *Electrochim. Acta* 36 (1991) 1191–1196.
- [11] B.T. Sun, M. Skyllas-Kazacos, *Electrochim. Acta* 36 (1991) 513–517.
- [12] B.T. Sun, M. Skyllas-Kazacos, *Electrochim. Acta* 37 (1992) 1253–1260.
- [13] B.T. Sun, M. Skyllas-Kazacos, *Electrochim. Acta* 37 (1992) 2459–2465.
- [14] X.G. Li, K.L. Huang, S.Q. Liu, N. Tan, L.Q. Chen, *Trans. Nonferrous Met. Soc. China* 17 (2007) 195–199.
- [15] Z. González, A. Sánchez, C. Blanco, M. Granda, R. Menéndez, R. Santamaría, *Electrochem. Commun.* 13 (2011) 1379–1382.
- [16] Y. Lu, W. Li, F. Sun, L. Zhao, L. Xing, *Carbon* 48 (2010) 3079–3090.
- [17] W.Y. Li, J.G. Liu, C.W. Yan, *Carbon* 49 (2011) 3463–3470.
- [18] C.G. Granqvist, E. Avendano, A. Azens, *Thin Solid Films* 442 (2003) 201–211.
- [19] C. Santato, M. Odziemkowski, M. Ulmann, J. Augustynski, *J. Am. Chem. Soc.* 123 (2001) 10639–10649.
- [20] M. Stankova, X. Vilanova, J. Calderer, E. Llobet, P. Ivanov, I. Gracia, C. Cane, X. Correig, *Sens. Actuators, B: Chem.* 102 (2004) 219–225.
- [21] L.X. Yang, C. Bock, B. MacDougall, J. Park, *J. Appl. Electrochem.* 34 (2004) 427–438.
- [22] R.S. Roth, J.L. Waring, Phase equilibria as related to crystal structure in the system niobium pentoxide–tungsten trioxide, *J. Res. Natl. Bur. Stand., Sect. A* 70 (1966) 281–303.
- [23] Y. Wu, *Basis of Applied Catalysis*, Chemical Industry Press, Beijing, 2008, pp. 369–397.